haematologica
Journal of The Ferrata Storti Foundation

Preclinical development of a humanized chimeric antigen receptor against B cell maturation antigen for multiple myeloma

by Lorena Perez-Amill, Guillermo Suñe, Asier Antoñana-Vildosola, Maria Castella, Amer Najjar, Jaume Bonet, Narcis Fernández-Fuentes, Susana Inogés, Ascensión López, Clara Bueno, Manel Juan, Alvaro Urbano-Ispizua, and Beatriz Martín-Antonio

Haematologica 2020 [Epub ahead of print]

Citation: Lorena Perez-Amill, Guillermo Suñe, Asier Antoñana-Vildosola, Maria Castella, Amer Najjar, Jaume Bonet, Narcis Fernández-Fuentes, Susana Inogés, Ascensión López, Clara Bueno, Manel Juan, Alvaro Urbano-Ispizua, and Beatriz Martín-Antonio. Preclinical development of a humanized chimeric antigen receptor against B cell maturation antigen for multiple myeloma. Haematologica. 2020; 105:xxx doi:10.3324/haematol.2019.228577

Preclinical development of a humanized chimeric antigen receptor against B cell maturation antigen for multiple myeloma

Lorena Perez-Amill[1], Guillermo Suñe[1], Asier Antoñana-Vildosola[1], Maria Castella[1], Amer Najjar[2], Jaume Bonet[3], Narcis Fernández-Fuentes[4], Susana Inogés[5], Ascensión López[5], Clara Bueno[6], Manel Juan[7], Alvaro Urbano-Ispizua[1,8,9] Beatriz Martín-Antonio[1,8]

[1] Department of Hematology, Hospital Clinic, IDIBAPS, Barcelona, Spain.
[2] Department of Pediatrics - Research, The University of Texas M. D. Anderson Cancer Center, Houston, TX, USA.
[3] Laboratory of Protein Design and Immunoengineering, École Polytechnique Fédérale de Lausanne, Lausanne, Switzerland.
[4] Department of Biosciences, U Science Tech. Universitat de Vic-Universitat Central de Catalunya, Spain.
[5] Department of Hematology and Cell Therapy Area and Department of Immunology and Immunotherapy, Clinic Universitary of Navarra, Navarra, Spain.
[6] Josep Carreras Leukemia Research Institute and Cell Therapy Program of the School of Medicine, University of Barcelona. Barcelona, Spain.
[7] Department of Immunotherapy, Hospital Clinic, IDIBAPS, Barcelona, Spain.
[8] Josep Carreras Leukaemia Research Institute, Barcelona, Spain.
[9] Department of Hematology, University of Barcelona, Barcelona, Spain.

Classification: Immunotherapy
Correspondence should be addressed to: Beatriz Martin-Antonio, PhD
bmartina@clinic.cat

Department of Hematology, Hospital Clinic, IDIBAPS/Josep Carreras Leukaemia Research Institute
Carrer Rosselló 149-153, 08036. Barcelona. Spain
Ph: +34-93 227 45 28 FAX: +34-93 312 94 07

Abstract word count: 228
Text word count: 4000
Figures: 7
Tables: 0
Reference count: 48

Running title: CAR-BCMA for multiple myeloma
Keywords: CART cells, Multiple myeloma, cytokine release syndrome, BCMA

Abstract

Multiple myeloma is a prevalent and incurable disease, despite the development of new and effective drugs. The recent development of chimeric antigen receptor (CAR)-T cell therapy has shown impressive results in the treatment of patients with relapsed or refractory hematological B cell malignancies. In the recent years, B-cell maturation antigen (BCMA) has appeared as a promising antigen to target using a variety of immunotherapy treatments including CART cells, for MM patients. To this end, we generated clinical-grade murine CART cells directed against BCMA, named ARI2m cells. Having demonstrated its efficacy, and in an attempt to avoid the immune rejection of CART cells by the patient, the single chain variable fragment was humanized, creating ARI2h cells. ARI2h cells demonstrated comparable *in vitro* and *in vivo* efficacy to ARI2m cells, and superiority in cases of high tumor burden disease. In terms of inflammatory response, ARI2h cells showed a lower TNFα production and lower *in vivo* toxicity profile. Large-scale expansion of both ARI2m and ARI2h cells was efficiently conducted following Good Manufacturing Practice guidelines, obtaining the target CART cell dose required for treatment of multiple myeloma patients. Moreover, we demonstrate that soluble BCMA and BCMA released in vesicles impacts on CAR-BCMA activity. In summary, this study sets the bases for the implementation of a clinical trial (EudraCT code: 2019-001472-11) to study the efficacy of ARI2h cell treatment for multiple myeloma patients.

Introduction

Multiple myeloma (MM) remains an incurable hematologic malignancy [1] responsible for 15-20% of all hematological malignancies [1, 2] with an average increase of 0.8% of new cases each year over the past decade [3]. The natural history of MM is relapse until refractory disease without reaching a plateau of survival with less than 10% of patients achieving sustained complete remission (CR) beyond 5-10 years after autologous stem-cell transplantation (ASCT) [4]. Moreover, patients are rarely cured after high-dose chemotherapy followed by ASCT indicating that novel strategies are required to improve the survival of relapsed/refractory (R/R) MM patients.

In the recent years, chimeric antigen receptor (CAR)T cell immunotherapy, based on the infusion of genetically modified autologous T cells to recognize an antigen expressed on the tumor cell, has changed the modality of treatment for certain hematological malignancies. Specifically, in acute lymphoblastic leukemia (ALL) and lymphomas targeting CD19 using CART cells has achieved outstanding responses [5-8]. In MM, B cell maturation antigen (BCMA) [9-11], has appeared as the most promising target for CART cell immunotherapy.

Clinical studies in R/R MM patients receiving CART-BCMA cells have demonstrated outstanding responses [12]. Unfortunately patients end-up relapsing [12, 13]. Interestingly, in comparison to CART19, a higher CART cell dose is required to achieve responses, being $150x10^6$ of CART cells the lowest dose required to obtain response in R/R patients to a median of 7 lines of treatment [12, 14]. Moreover, it has been shown that a deepening of the response is obtained over time [12]. In addition, the use of humanized or human CARs instead of murine CARs is appearing as the current trend in CART cell immunotherapy [15, 16].

Here, using the same structure developed for a CAR19 (ARI-0001), a CAR that has already been used in a Phase I clinical trial (NCT03144583) for B cell malignancies at our institution [17], we generated an academic murine CAR against BCMA (ARI2m) and a humanized version (ARI2h). The efficacy and inflammatory response of both ARI2m and ARI2h cells were compared. Both CART cells showed a comparable anti-MM activity. However, a higher efficacy for ARI2h cells in cases of high tumor burden was observed. Also, the feasibility of clinical-grade expansion was tested in parallel in two different institutions and successfully achieved for both CARs. Finally, the impact of soluble BCMA (sBCMA) in ARI2m cells activity was analyzed demonstrating how sBCMA can negatively impact the CAR-BCMA activity. Taken together, this study sets the bases for a multicenter Clinical Trial for MM patients with ARI2h cells in Spain (EudraCT code: 2019-001472-11).

Methods

Ethics Statement: Research involving human materials was approved by Ethical Committee of Clinical Research (Hospital Clinic, Barcelona). Peripheral blood (PB) T cells were obtained from healthy donors after informed consent. All animal work was performed under the Ethical Committee of Animal Research (Hospital Clínic, Barcelona).

Cloning and humanization strategy: anti-BCMA scFv was designed from J22.9 antibody [18]. Human CD8a domains, 4-1BB and CD3ζ domains were obtained from the CART19 used at our Institution [17]. Anti-CD19 scFv was substituted for the anti-BCMA scFv of J22.9 antibody. To obtain ARI2h, the scFv sequence of J22.9 antibody was humanized using two predictive models (Blast and Germline). Selected amino acids (excluding Complementarity-Determining Region (CDR) and Vernier zone) were substituted for their homologous sequence in humans.

Predictive *in silico* models: immunogenicity against MHC-I was predicted with NetMHC-4.0 [19-21] as previously described [15]. In detail, binding affinities of every 9-mer peptides from both scFv that are not encoded by the human genome were evaluated for 12 HLA-I alleles (5 type A and 7 type B) to predict binding affinity. As humanized ARI2h scFv contains human framework regions, only sub-peptides from CDRs and Vernier zone were considered. The affinity threshold to select only strong binders was <100nM. Binding affinity: structural models derived for each antibody-BCMA pair were built with M4T [22] using the crystal structure of the J22.9xi-BCMAhuman complex (4ZFO) [18] from the Protein Data Bank [23] as template. The quality and stereochemistry of the model was assessed using Prosa-II [24] and PROCHECK [25] respectively. For each structural complex antibody-antigen model a total of 100 minimization trajectories were performed, followed by an estimation of the binding affinity as the energy difference between the complex and its separated components (ddG). Minimization and ddG analysis were carried out with Rosetta Design Suite [26, 27]. The quality of the binding affinity model was very high [28] due to the high level of sequence identity between target sequences and template showing similar protein-protein interfaces (Supplementary Figure 1D).

Clinical grade production of ARI2 cells: Lentiviral particles were produced inside a clean room facility following GMP guidelines as previously described [17]. ARI2h/ARI2m cells clinical-grade were produced using CliniMACS Prodigy (Miltenyi, Biotec) as previously described [17].

See also Supplementary Methods.

Results

ARI2m cells demonstrate potent anti-myeloma activity

ARI2m sequence (Supplementary Figure 1A) contains the scFv sequence of the anti-BCMA antibody J22.9 [18], which has been shown to be effective against MM [29], and human CD8a, 4-1BB and CD3ζ as hinge, transmembrane, co-stimulatory and signaling domains (Figure 1A). CART cell transfection efficiencies varied between 30-60% in different experiments. CAR expression was retained after cryopreservation (Supplementary Figure 1B). ARI2m cells efficacy was tested against ARP1 and U266 MM cells by co-culturing T cells and MM cells at an E:T ratio of 1:1 over four days. ARI2m cells efficiently eliminated MM cells in comparison to UT T cells (Figure 1B) while no cytotoxicity was observed against a BCMA-negative cell line (K562) demonstrating specificity of ARI2m cells (Figure 1B). In addition, limiting dilution cytotoxicity assays from 1:1 to 0.125 E:T ratios demonstrated a high efficacy of ARI2m cells by eliminating MM cells at a low E:T ratio at 36h (Figure 1C), which continued to increase at 72h (Supplementary Figure 1C).

The production of pro-inflammatory cytokines by ARI2m cells was analyzed after co-culturing ARI2m cells and MM cells at different E:T ratios, at 24 and 48h. A high IFNγ production was observed at 24h which increased at 48h (Figure 1D). Some IFNγ production was detected for UT T cells as expected, as UT T cells are activated during *in vitro* expansion. Minimum levels of IL6 were detected at 24h which increased at 48h (Figure 1D). TNFα production decreased at 48h in comparison to 24h suggesting that TNFα is produced at early times of CART activation (Figure 1D).

In vivo efficacy of ARI2m cells was analyzed in a murine model where NSG-mice received $1x10^6$ of ARP1 MM cells. Mice were treated 6 days later with either $10x10^6$ of UT cells or $10x10^6$ of T cells containing $2x10^6$ of ARI2m cells (Figure 1E). ARI2m cells prevented disease progression and performed better than UT T cells (Figure 1E-1F). As expected, this translated into an increased survival (Figure 1G). Furthermore, analysis of mice tissues at experimental end-point showed absence of MM cells in BM and spleen (Figure 1H). T cells were mainly in the spleen (Figure 1I), whereas CART cells proliferated mainly in BM, as indicated by a higher percentage of CART cells from the whole T cell population in BM than in spleen (Figure 1I). Moreover, sBCMA was analyzed as an additional marker for MM progression in mice serum. As expected, a high amount of sBCMA was detected in mice treated with UT T cells while no sBCMA was found in mice treated with ARI2m cells (Figure 1J).

Humanization of ARI2m does not change affinity binding against human BCMA and enhances cytotoxicity against highly advanced myeloma disease

Early disappearance of CART cells [15] is associated with a xenorecognition of the murine component of the CAR scFV by the human immune system. To circumvent this problem, we designed a humanized sequence of the scFv of ARI2m (Supplementary Figure 1A). Two different humanized variants were created based on two different predictive algorithms (Blast and Germline) by substitution of amino acids of the variable regions of heavy and light chains. *In vitro* comparison of efficacy of both variants demonstrated that Germline variant had a slightly higher anti-MM activity (Figure 2A) and equal specificity, since none of them eliminated K562 cells (Figure 2A). Therefore, Germline variant, which was termed ARI2h, was selected for additional characterization. Predictive *in silico* models for immunogenicity of both scFv demonstrated higher immunogenicity for ARI2m than ARI2h (Figure 2B). Then, binding affinity prediction of both scFv against murine and human BCMA showed that both scFv bind to human BCMA with similar affinity while being

unable to bind mouse BCMA (Figure 2C). Structural comparison between both scFv showed that most structural changes during the humanization were concentrated in the heavy chain of the antibody. CDR regions on the antibody included no mutations and presented almost no structural drift (Figure 2D), reinforcing the idea that both antibodies presented an almost identical binding surface. Afterwards, we analyzed whether T cell transfection with either ARI2m or ARI2h CAR constructs would lead to different phenotypes in ARI2 cells. We did not observe any difference neither in the proportion of ARI2+CD4 and ARI2+CD8 cell populations (Figure 2E) nor in the proportion of memory T cell subsets (Supplementary Figure 1E).

Moreover, as a slightly lower *in vitro* efficacy of ARI2h *vs* ARI2m cells was noticed (Figure 2A), a long-term cytotoxicity assay was performed by co-culturing tumor and ARI2 cells at low E:T (0.125:1) ratio. This assay showed slower killing kinetics for ARI2h cells, but an equal anti-MM activity at longer time-points (Figure 2F). Accordingly, T cell proliferation upon CAR-antigen binding was slower for ARI2h cells (Figure 2G). In addition, whereas the same level of IFNγ was produced by both CART cells, a lower TNFα and similar IL6 production was detected for ARI2h cells (Figure 2H).

Anti-MM activity of ARI2h and ARI2m cells was further evaluated using two different *in vivo* models of MM (early and advanced disease models). Mice received MM cells on day 0 and were treated with $5x10^6$ of CART cells either on day 6 or 14 to create an early and advanced model of disease, respectively (Figure 3A-3B). In the early disease model, ARI2h and ARI2m cells equally prevented MM progression (Figure 3A and 3C). Around day 50, mice started to show signs of toxicity, which was more severe in the ARI2m group and translated into lower survival for this group (Figure 3D). These results suggested that toxicity was related to a global higher number of T cells proliferating in the ARI2m-treated group, as previously observed [30]. In the advanced disease model, whereas ARI2m abrogated disease progression completely, minimal levels of MM disease were detected in the ARI2h group at certain time points (Figure 3B) although this difference was not significant (Figure 3C). Interestingly, mice treated with ARI2h cells showed again an increased survival consistent with lower toxicity in comparison to ARI2m cells (Figure 3D). Accordingly, in both disease models, the global number of T cells was higher for ARI2m than for ARI2h cells (Figure 3E), which might explain the higher xeno-GVHD observed in the ARI2m-treated group. Importantly, majority of T cells in BM corresponded to CART cells, for both ARI2m and ARI2h cells, and in both disease models (Figure 3E). Lastly, mice serum analysis showed that both CARs secreted high amounts of IFNγ. However, and in agreement with previous observations of a slower kinetics for ARI2h cells, IFNγ production was slower in the ARI2h group. Thus, in the early model, IFNγ could not be detected in the ARI2h group 3 days after CART infusion but was higher at day 31 (Figure 3F). Similarly, in the advanced disease model, no IFNγ was detected at day 5 for ARI2h cells, but levels increased at day 21 (Figure 3F).

These results suggested a faster activity of ARI2m *vs* ARI2h cells, which in cases of high tumor burden, might lead to faster CART cell exhaustion and their disappearance. To test this hypothesis, a third *in vivo* experiment with a lower CART cell dose ($3x10^6$) was performed. Disease burden was higher at the time of CART cell injection compared to previous experiments (Figure 3B *vs* Figure 4A). In this model, neither ARI2m nor ARI2h cells could avoid disease progression (Figure 4B). However, ARI2h cells performance was better than ARI2m cells slowing disease progression (Figure 4B). At final time point, when mice were euthanized due to disease progression and not to xeno-GVHD, T cells in mice at the time of sacrifice were almost undetectable (Figure 4C). However, mice treated with ARI2h cells presented higher number of ARI2h cells in BM (Figure 4C). This data suggests that slower CART proliferation could lead to longer CART cell persistence and superior anti-tumor activity in cases of high tumor burden. To further support

these findings, we exposed both ARI2m and ARI2h cells to consecutive *in vitro* challenges with MM (Figure 4D). In agreement with the lower ARI2m efficacy observed under high tumor burden disease, these experiments demonstrated more durable persistence for CD4 and CD8-ARI2h cells, which was not consistent for ARI2m cells (Figure 4E).

ARI2h cells induce lower TNFα production than ARI2m cells

Previous studies have shown that macrophages, after being activated by CART cells, are the main producers of IL6, IL1β and TNFα [31, 32] which leads to cytokine release syndrome (CRS) development in patients. Therefore, to further analyze the pro-inflammatory profile of both CARs we established an *in vitro* system adding macrophages. Thus, co-cultures of effector and target cells were conducted in the presence of macrophages (Figure 5A). Macrophages addition did not affect CART cell cytotoxicity (Figure 5B). IFNγ was only slightly increased but a very significant increase was detected for IL6, TNFα and IL1β, the last one not being detected in the absence of macrophages (Figure 5C). Next, we compared the pro-inflammatory activity of ARI2m cells and ARI2h cells over two days using this setting. We observed similar IFNγ, IL6 and IL1β production for both CARs (Figure 5D) but TNFα production was lower for ARI2h cells, consistent with the long-term *in vitro* assay previously performed (Figure 2H) and the lower *in vivo* toxic activity for ARI2h compared to ARI2m cells.

Efficient clinical production and activity of ARI2 cells

Pre-clinical data presented here supports the development of a Phase I Multicenter Clinical Trial for MM patients (EudraCT code: 2019-001472-11) to evaluate the efficacy of ARI2 cells. The feasibility of large-scale, clinical-grade production was tested both for ARI2m and ARI2h cells using T cells from healthy donors. CART cell production system has been previously established at our institution and being used in an ongoing phase I clinical trial with a CAR19 product (ARI-0001) [17]. Four expansions were conducted for each CAR in two different institutions. Both ARI2m and ARI2h cells were efficiently expanded and the required CART cell dose (>150x10^6 CART cells) [12] was achieved in all cases (Figure 6A and 6B). Anti-MM activity for both ARI2h and ARI2m cells was also demonstrated (Figure 6C). In both institutions, all productions achieved the minimum threshold required for product release (Figure 6D and 6E).

Soluble and released BCMA impacts ARI2 cells activity

Clinical studies with CART19 in ALL have shown that 1x10^6 CARTcells/kg is sufficient to achieve CR [5]. In MM however a higher dose is needed (>150x10^6) [12]. BCMA is cleaved and released as soluble BCMA (sBCMA) into the extracellular milieu [33]. We hypothesized that sBCMA can bind to CAR-BCMA, partially hampering its anti-MM activity, thereby explaining the high CAR-BCMA dose required to achieve CR in MM patients. Therefore, we measured the amount of sBCMA in serum of patients with monoclonal gammopathy of undetermined significance, in newly diagnosed MM patients and at relapse. As expected, we observed higher amount of sBCMA in MM patients (Figure 7A).

To test whether sBCMA inhibits CART activity, MM cells were co-cultured with ARI2m cells in the presence of recombinant BCMA protein. Results confirmed that recombinant BCMA blocks ARI2m cells activity in terms of cytotoxicity and IFNγ production (Figure 7B). As MM patients presented around 100 ng/mL of sBCMA, a titration assay with recombinant BCMA demonstrated an inhibition of ARI2m cells activity up to 32 ng/mL of BCMA (Figure 7C). BCMA shedding is mediated by γ-secretase, which directly cleaves and

releases BCMA into the milieu decreasing surface BCMA expression. Therefore, BCMA shedding can be blocked using γ-secretase inhibitors [33]. To analyze the effect of a γ-secretase inhibitor (DAPT), we measured membrane bound BCMA in MM cells and the amount of sBCMA before and after treating MM cells with DAPT. As expected, DAPT treatment increased BCMA surface expression in MM cells and decreased release of sBCMA (Figure 7D and 7E). Increase in membrane-bound BCMA and decreased sBCMA associated to DAPT treatment was also detected after co-culturing MM cells with UT T cells (Figure 7D and 7E). In the case of ARI2m/MM cells co-culture, DAPT addition decreased the amount of sBCMA, as expected. However, membrane-bound BCMA was poorly detected due to the high ARI2m cells *in vitro* activity eliminating MM cells (Figure 7D and 7E). Having demonstrated that DAPT treatment prevents BCMA shedding, we tested whether this effect results on enhanced ARI2m cells activity. This analysis was conducted in transwell plates, where untouched MM cells were placed in the upper well and ARI2m-MM cells co-culture in the lower well (Figure 7F). In this setting, MM cells in the upper well are continuously releasing sBCMA. Cytotoxicity assay showed reduced ARI2m cells cytotoxicity and IFNγ production in the presence of sBCMA (with MM cells in the upper well), compared to the control without MM cells in the upper well (Figure 7G). Moreover, DAPT addition in this transwell assay enhanced the cytotoxicity and IFNγ production of ARI2m cells without impacting the proliferation of ARI2m cells (Figure 7G).

In addition, using confocal fluorescence microscopy we observed that BCMA is released from MM cells in vesicles (Figure 7H) in a mechanism that could also reduce CART cell activity. Therefore, to confirm that these BCMA vesicles could impact temporarily CAR-BCMA activity, MM cells over-expressing BCMA fused to GFP (MM-BCMA-GFP) were co-cultured with ARI2m cells for 3 hours and time-lapse *in vivo* imaging was performed. We confirmed that BCMA released in vesicles bind to ARI2m cells distracting ARI2m cells from their target MM cells (Figure 7I and Supplementary Movie 1). Moreover, we also observed that ARI2m cells after contacting MM cells could acquire in their membranes BCMA from the surface of MM cells, and as a consequence, fratricide was observed between ARI2m cells (Figure 7J and Supplementary Movie 2). To further confirm this event, ARI2m and MM cells co-cultured in presence of a trogocytosis inhibitor (LatrunculinA) showed decreased % of BCMA acquisition for ARI2m cells (Figure 7K). In addition, ARI2m cells after acquiring BCMA in their membranes showed decreased anti-MM activity (Figure 7L).

Discussion

BCMA was identified in 2013 [10] as the most promising antigen for CART cell immunotherapy for the treatment of R/R MM patients, a finding which was confirmed in different clinical studies in MM patients [12, 13] and led us to develop our murine CAR-BCMA cells with 4-1BB as co-stimulatory domain (ARI2m cells). ARI2m cells demonstrated a high anti-MM activity which is retained in their humanized version (ARI2h cells). Additionally, a higher efficacy of ARI2h *vs* ARI2m cells was observed *in vivo* in mice with high tumor burden. Our results set the bases for a multicenter Phase I/II Clinical Trial for R/R MM patients with ARI2h cells in Spain.

The success of BCMA as a target for CART cell immunotherapy was demonstrated for first time in patients with a CAR-BCMA with CD28 as co-stimulatory domain. However, this CAR displayed high toxicity [14]. Therefore, CD28 was replaced by 4-1BB, and the new CAR (bb2121) demonstrated manageable toxicity and that a minimum dose of $150x10^6$ CART cells is required to obtain responses [12]. In parallel, two additional studies [13, 34], demonstrated that a lower number of previous treatments led to better responses, and that short-term CAR T cell expansion is more consistent after lymphodepletion [34]. Different factors influence CART cell expansion and persistence that will enhance the long-term control of the disease [5, 12, 13, 34], a factor that needs to be improved with CAR-BCMA therapy, as a high number of MM patients end-up relapsing [12, 13]. One of the suggested reasons for this is the limited persistence of CART cells. In this regard, human or humanized CARs by avoiding the immunological reaction of the human immune system against the murine components of the scFv of the CAR might increase the persistence of CART cells [15, 16, 30]. Based on these previous studies, and supported by our results showing that both ARI2m and ARI2h cells equally avoided disease progression, we selected ARI2h cells, which are humanized CAR-BCMA cells, to be used for a clinical trial for MM patients (EudraCT code: 2019-001472-11).

Moreover, long-term CART cell persistence associate with durability of remission [5, 12, 13, 34]. Factors impacting on long-term CART cell persistence include the exhaustion profile of CART cells [29, 35] and the affinity for the target antigen in combination with the co-stimulatory domain of CART cells. In this regard, studies in CART19 with CD28 and 4-1BB have demonstrated that a strong activation of CART cells, due to high affinity or high expression of the target antigen combined with CD28 domain, leads to faster CART cell proliferation with increased exhaustion and shorter persistence. On the contrary, slower CART activation, due to lower affinity to the target antigen or to 4-1BB domain, reduces exhaustion improving persistence [35-376, 38, 39]. Here, even though ARI2m and ARI2h cells had 4-1BB co-stimulatory domain and presented the same affinity against human BCMA, ARI2h cells had slower kinetic activity, and demonstrated higher efficacy than ARI2m cells in a high tumor burden disease murine model and higher persistence after consecutive challenges to tumor cells.

A high incidence of CRS and neurotoxicity are common events occurring after CART cell administration [5, 12, 13, 34, 40-42]. Although they are efficiently managed following international guidelines [43, 44], the ideal CART treatment should try to minimize CRS development. Here, the use of ARI2h cells instead of ARI2m is further supported by the observation of lower TNFα *in vitro* production of ARI2h cells. Whereas IL6 is the effector cytokine for CRS [31, 45, 46] which exponentially increases as CRS develops, other cytokines such as TNFα and IL1β [31, 32] are the main initiators of CRS, as they are produced at early time points by monocytes and macrophages once they are activated by IFNγ produced by CART cells. In fact, TNFα, acts as an initiator cytokine orchestrating the cytokine cascade in many inflammatory diseases appearing as a therapeutic

target for inflammatory diseases [46]. Here, our *in vitro* model with macrophages mimicking a more similar model to the *in vivo* scenario, demonstrates that ARI2h cells induced lower TNFα production by macrophages, a relevant finding, as CRS in MM patients after CAR-BCMA treatment associates with a higher peak of TNFα [12]. Moreover, CARs with a faster kinetic associate with higher CRS [37], suggesting that the slower kinetics of ARI2h cells in comparison to ARI2m cells might also explain the lower *in vivo* toxicity observed.

Last, here, the impact of sBCMA on CART activity was analyzed. Even though studies with CAR-BCMA in MM have not found any correlation between sBCMA and CART activity [10, 12, 34, 47], we observed that the high *in vitro* CART activity rapidly eliminating MM cells impedes to analyze properly the role of sBCMA in preclinical studies. Our *in vitro* models performed at a low CAR-BCMA:MM ratio, with the creation of an environment with continuous release of sBCMA, and the addition of a γ-secretase inhibitor confirmed the negative impact of sBCMA on CAR-BCMA activity. Moreover, we observed that BCMA is also released in vesicles structures distracting CART cells from their targets, and that BCMA can be transferred to CART cells in a mechanism which appears trogocytosis, a finding already observed for CART19 cells [48], causing decreased ARI2m cells anti-MM activity.

In conclusion, we have developed CAR-BCMA cells with 4-1BB as co-stimulatory domain that have been humanized retaining high efficacy and demonstrating a lower toxicity than their murine counterpart. ARI2 cells can be efficiently expanded under GMP conditions for its use in a clinical trial. Moreover, we demonstrate that sBCMA and released BCMA from MM cells can impact CART activity.

Funding: Celgene and Institute of Health Carlos III (project: PI17/01043) provided funding for all *in vitro* and *in vivo* studies.

Authorship Contributions: LPA and BMA designed the study, LPA performed *in vitro* and *in vivo* experiments. GS: performed clonings, virus production and *in vivo* experiments. LPA and BMA analyzed data and wrote the manuscript. AN designed the scFv of ARI2m and provided viral vector for GFP-Ffluc. MC and AA provided advice for experiments. AA performed some of the CART *in vitro* expansions. MJ, SI and AL performed clinical grade ARI2 production. JB and NFF performed predictive models for binding affinity. CB performed cell sortings. AUI provided funding and constructive ideas. All authors reviewed the manuscript.

Acknowledgements: We acknowledge Multiple Myeloma Research Center (Little Rock, AK) for providing ARP1 cell line. We acknowledge the facilities of Confocal Fluorescence Microscopy at the University of Barcelona. We declare no conflicts of interests.

References:

1. Palumbo A, Anderson K. Multiple myeloma. N Engl J Med. 2011;364(11):1046-1060.
2. Kumar SK, Callander NS, Alsina M, et al. Multiple Myeloma, Version 3.2017, NCCN Clinical Practice Guidelines in Oncology. J Natl Compr Canc Netw. 2017;15(2):230-269.
3. Cancer Stat Facts: Myeloma. National Cancer Institute Surveillane, Epidemiology, and End Results Program Web site. Avilable at http://seercancergov/statfacts/html/mulmyhtml. 2017;
4. Martinez-Lopez J, Blade J, Mateos MV, et al. Long-term prognostic significance of response in multiple myeloma after stem cell transplantation. Blood. 2011;118(3):529-534.
5. Maude SL, Laetsch TW, Buechner J, et al. Tisagenlecleucel in Children and Young Adults with B-Cell Lymphoblastic Leukemia. N Engl J Med. 2018;378(5):439-448.
6. Schuster SJ, Svoboda J, Chong EA, et al. Chimeric Antigen Receptor T Cells in Refractory B-Cell Lymphomas. N Engl J Med. 2017;377(26):2545-2554.
7. Park JH, Riviere I, Gonen M, et al. Long-Term Follow-up of CD19 CAR Therapy in Acute Lymphoblastic Leukemia. N Engl J Med. 2018;378(5):449-459.
8. Neelapu SS, Locke FL, Bartlett NL, et al. Axicabtagene Ciloleucel CAR T-Cell Therapy in Refractory Large B-Cell Lymphoma. N Engl J Med. 2017;377(26):2531-2544.
9. O'Connor BP, Raman VS, Erickson LD, et al. BCMA is essential for the survival of long-lived bone marrow plasma cells. J Exp Med. 2004;199(1):91-98.
10. Carpenter RO, Evbuomwan MO, Pittaluga S, et al. B-cell maturation antigen is a promising target for adoptive T-cell therapy of multiple myeloma. Clin Cancer Res. 2013;19(8):2048-2060.
11. Novak AJ, Darce JR, Arendt BK, et al. Expression of BCMA, TACI, and BAFF-R in multiple myeloma: a mechanism for growth and survival. Blood. 2004;103(2):689-694.
12. Raje N, Berdeja J, Lin Y, et al. Anti-BCMA CAR T-Cell Therapy bb2121 in Relapsed or Refractory Multiple Myeloma. N Engl J Med. 2019;380(18):1726-1737.
13. Zhao WH, Liu J, Wang BY, et al. A phase 1, open-label study of LCAR-B38M, a chimeric antigen receptor T cell therapy directed against B cell maturation antigen, in patients with relapsed or refractory multiple myeloma. J Hematol Oncol. 2018;11(1):141.
14. Ali SA, Shi V, Maric I, et al. T cells expressing an anti-B-cell maturation antigen chimeric antigen receptor cause remissions of multiple myeloma. Blood. 2016;128(13):1688-1700.
15. Sommermeyer D, Hill T, Shamah SM, et al. Fully human CD19-specific chimeric antigen receptors for T-cell therapy. Leukemia. 2017;31(10):2191-2199.
16. Turtle CJ, Hanafi LA, Berger C, et al. CD19 CAR-T cells of defined CD4+:CD8+ composition in adult B cell ALL patients. J Clin Invest. 2016;126(6):2123-2138.
17. Castella M, Boronat A, Martin-Ibanez R, et al. Development of a Novel Anti-CD19 Chimeric Antigen Receptor: A Paradigm for an Affordable CAR T Cell Production at Academic Institutions. Mol Ther Methods Clin Dev. 2018;12:134-144.
18. Oden F, Marino SF, Brand J, et al. Potent anti-tumor response by targeting B cell maturation antigen (BCMA) in a mouse model of multiple myeloma. Mol Oncol. 2015;9(7):1348-1358.
19. Lundegaard C, Lamberth K, Harndahl M, Buus S, Lund O, Nielsen M. NetMHC-3.0: accurate web accessible predictions of human, mouse and monkey MHC class I affinities for peptides of length 8-11. Nucleic Acids Res. 2008;36(Web Server issue):W509-512.
20. Andreatta M, Nielsen M. Gapped sequence alignment using artificial neural networks: application to the MHC class I system. Bioinformatics. 2016;32(4):511-517.
21. Nielsen M, Andreatta M. NetMHCpan-3.0; improved prediction of binding to MHC class I molecules integrating information from multiple receptor and peptide length datasets. Genome Med. 2016;8(1):33.

22. Fernandez-Fuentes N, Madrid-Aliste CJ, Rai BK, Fajardo JE, Fiser A. M4T: a comparative protein structure modeling server. Nucleic Acids Res. 2007;35(Web Server issue):W363-368.
23. Berman HM, Westbrook J, Feng Z, et al. The Protein Data Bank. Nucleic Acids Res. 2000;28(1):235-242.
24. Sippl MJ. Recognition of errors in three-dimensional structures of proteins. Proteins. 1993;17(4):355.
25. Laskowski RA, MacArthur MW, Moss DS, Thornton J. PROCHECK: a program to check the sterochemical quality of protein structures. J Appl Cryst. 1993;26:283-291.
26. Fleishman SJ, Leaver-Fay A, Corn JE, et al. RosettaScripts: a scripting language interface to the Rosetta macromolecular modeling suite. PLoS One. 2011;6(6):e20161.
27. Leaver-Fay A, Tyka M, Lewis SM, et al. Chapter nineteen - Rosetta3: An Object-Oriented Software Suite for the Simulation and Design of Macromolecules. Methods Enzymol. 2011;487:545-574.
28. Baker D, Sali A. Protein structure prediction and structural genomics. Science. 2001;294(5540):93-96.
29. Bluhm J, Kieback E, Marino SF, et al. CAR T Cells with Enhanced Sensitivity to B Cell Maturation Antigen for the Targeting of B Cell Non-Hodgkin's Lymphoma and Multiple Myeloma. Mol Ther. 2018;26(8):1906-1920.
30. Smith EL, Staehr M, Masakayan R, et al. Development and Evaluation of an Optimal Human Single-Chain Variable Fragment-Derived BCMA-Targeted CAR T Cell Vector. Mol Ther. 2018;26(6):1447-1456.
31. Giavridis T, van der Stegen SJC, Eyquem J, Hamieh M, Piersigilli A, Sadelain M. CAR T cell-induced cytokine release syndrome is mediated by macrophages and abated by IL-1 blockade. Nat Med. 2018;24(6):731-738.
32. Norelli M, Camisa B, Barbiera G, et al. Monocyte-derived IL-1 and IL-6 are differentially required for cytokine-release syndrome and neurotoxicity due to CAR T cells. Nat Med. 2018;24(6):739-748.
33. Laurent SA, Hoffmann FS, Kuhn PH, et al. gamma-Secretase directly sheds the survival receptor BCMA from plasma cells. Nat Commun. 2015;6:7333.
34. Cohen AD, Garfall AL, Stadtmauer EA, et al. B cell maturation antigen-specific CAR T cells are clinically active in multiple myeloma. J Clin Invest. 2019;129(6):2210-2221.
35. Salter AI, Ivey RG, Kennedy JJ, et al. Phosphoproteomic analysis of chimeric antigen receptor signaling reveals kinetic and quantitative differences that affect cell function. Sci Signal. 2018;11(544).
36. Long AH, Haso WM, Shern JF, et al. 4-1BB costimulation ameliorates T cell exhaustion induced by tonic signaling of chimeric antigen receptors. Nat Med. 2015;21(6):581-590.
37. Milone MC, Fish JD, Carpenito C, et al. Chimeric receptors containing CD137 signal transduction domains mediate enhanced survival of T cells and increased antileukemic efficacy in vivo. Mol Ther. 2009;17(8):1453-1464.
38. Wherry EJ, Kurachi M. Molecular and cellular insights into T cell exhaustion. Nat Rev Immunol. 2015;15(8):486-499.
39. Smith-Garvin JE, Koretzky GA, Jordan MS. T cell activation. Ann Rev Immunol. 2009;27:591-619.
40. Schuster SJ, Svoboda J, Chong EA, et al. Chimeric Antigen Receptor T Cells in Refractory B-Cell Lymphomas. N Engl J Med. 2017;377(26):2545-2554.
41. Locke FL, Neelapu SS, Bartlett NL, et al. Phase 1 Results of ZUMA-1: A Multicenter Study of KTE-C19 Anti-CD19 CAR T Cell Therapy in Refractory Aggressive Lymphoma. Mol Ther. 2017;25(1):285-295.
42. Shah N, Alsina M, Siegel DS, et al. Initial Results from a Phase 1 Clinical Study of bb21217, a Next-Generation Anti Bcma CAR T Therapy. Blood. 2018;132(Suppl 1):488.
43. Porter D, Frey N, Wood PA, Weng Y, Grupp SA. Grading of cytokine release syndrome associated with the CAR T cell therapy tisagenlecleucel. J Hematol Oncol. 2018;11(1):35.

44. Lee DW, Santomasso BD, Locke FL, et al. ASTCT Consensus Grading for Cytokine Release Syndrome and Neurologic Toxicity Associated with Immune Effector Cells. Biol Blood Marrow Transplant. 2019;25(4):625-638.
45. Hunter CA, Jones SA. IL-6 as a keystone cytokine in health and disease. Nat Immunol. 2015;16(5):448-457.
46. Parameswaran N, Patial S. Tumor necrosis factor-alpha signaling in macrophages. Crit Rev Eukaryot Gene Expr. 2010;20(2):87-103.
47. Friedman KM, Garrett TE, Evans JW, et al. Effective Targeting of Multiple B-Cell Maturation Antigen-Expressing Hematological Malignances by Anti-B-Cell Maturation Antigen Chimeric Antigen Receptor T Cells. Hum Gene Ther. 2018;29(5):585-601.
48. Hamieh M, Dobrin A, Cabriolu A, et al. CAR T cell trogocytosis and cooperative killing regulate tumour antigen escape. Nature. 2019;568(7750):112-116.

Figure legends:

Figure 1: ARI2m cells demonstrate potent *in vitro* and *in vivo* anti-myeloma activity. (**A**) Design of ARI2m. (**B**) Cytotoxicity assays of ARI2m against ARP1 and U266 (MM cell lines) and non-myeloma K562 cells performed from 24-96h. (**C**) Limiting dilution cytotoxicity assay against ARP1 and U266 performed at ratios from 1:1 to 0.125.1 (T cell: Tumor cell line) at 36h. (**D**) Cytokine profile of IFNγ, IL-6 and TNF-α after 24h and 48h of co-culturing T cells and ARP1 cells. (**E-J**) *In vivo* efficacy of ARI2m cells: (**E-F**): Diagram of experimental design and quantification of disease progression by weekly bioluminescence imaging and overall survival of the different group of mice (**G**). (**H**) Flow cytometry of bone marrow (BM) and spleen of mice at the end of the experiment. (**I**) Percentage of total T cells and CART cells in BM and spleen in mice treated with ARI2m. (**J**). Soluble BCMA (sBCMA) from mice serum after being treated with ARI2m or UT T cells. *p<0.05.

Figure 2: Humanization of ARI2m into ARI2h and comparison of affinity and immunogenicity of ARI2m *vs* ARI2h (see also Supplementary Figure 1): (**A**). Limiting dilution cytotoxicity assay of ARI2m *vs* both humanized versions (Blast and Germline). (**B**). Predicted affinities of 9-mer peptides derived from either ARI2m or ARI2h scFv against HLA-I. Total number of sites with predicted affinity <100nM is shown on the left, and specific interactions of HLA-I alleles with each 9 mer peptide of the scFv is shown on the right. (**C**). Estimation of the binding affinity of both scFv against human and murine BCMA. Difference in Gibbs free energy (ddg) between the complex and its separated components for each protein pair highlights the inability of any of the antibodies to target murine BCMA. (**D**). Local structural comparison between both scFv performed through RMSD. CDR positions are highlighted in green while sequence differences between the two antibodies are mapped in gray under the curve. Resolution of the template structure of the Ab is represented as a dashed line. The graphic shows low structural drift on the antibodies' CDRs between the two antibody variants. (**E**). Phenotype characterization of T cells transduced with either ARI2m or ARI2h CAR construct and after being expanded for 7 days (n=3). (**F**) Long-term cytotoxic assay comparing ARI2m *vs* ARI2h cells against ARP1 (MM) and K562 with its proliferation (**G**) and IFNγ, TNFα and IL1β production (**H**). *p<0.05.

Figure 3: *In vivo* efficacy of ARI2m cells and ARI2h cells: Mice received MM cells on day 0, and were treated at the indicated days. Disease progression followed by weekly bioluminescence in the early disease model (**A**) and advanced disease model (**B**) and its quantification, respectively (**C**). (**D**) Kaplan-Meier curve representing the overall survival of the different groups of mice. (**E**) Total CD3+T cells and percentage of ARI2 cells from CD3+ T cells population found in BM and spleen for both early and advanced disease models. (**F**) ELISA of IFNγ from mice serum at day 3 and 31 for the early disease model and at day 5 and 21 for the advanced disease model. *p<0.05

Figure 4: Humanization of ARI2m enhances cytotoxicity against highly advanced myeloma disease: (**A)** Schematic representation and images of *in vivo* experiment in mice receiving ARP1 MM cells and treated either with ARI2m or ARI2h cells. (**B**) Disease progression followed by weekly bioluminescence of experiment in (**A**). (**C**). Total CD3+T cells and percentage of ARI2 cells from CD3+ T cells population found in BM. (**D**) Graph showing scheme of consecutive challenges of CART cells to MM cells. (**E**) Percentage of CART cells in CD4 or CD8 T cell subsets after each challenge. *p<0.05. **p<0.0001.

Figure 5: ARI2h induces a lower TNFα production than ARI2m: (**A**) Schematic representation of monocytes and T cell isolation from the same buffy coat and its differentiation into macrophages, CART *in vitro* expansion and co-culture with MM cell lines. (**B**) Cytotoxicity and (**C**) production of IFNγ, IL6, TNFα and IL1β of ARI2m co-cultured with ARP1 cells with or without macrophages. (**D**) Cytokine production over 48h of IFNγ, IL6, TNFα and IL1β after co-culturing ARI2m/ARI2h with macrophages and ARP1 MM cells. Macrophages were added at a 1:3 ratio macrophage:CART. *p<0.05. **p<0.0001.

Figure 6: Efficient clinical productions and activities of ARI2m and ARI2h cells: (**A** and **B**): Clinical expansion of ARI2m and ARI2h cells showing the total T cells (**A**) and the total CART cell number (**B**) achieved at the end of the expansion. (**C**). Cytototoxicy assays against U266 MM cell line of both ARI2m and ARI2h cells at the end of the expansion. Results from A-C show median of four clinical expansions of ARI2m and ARI2h cells. (**D-E**). Detailed comparison of the four clinical productions performed in two different institutions, showing the percentage of each cell population achieved (**D**) and the specified parameters for product release (**E**).. *p<0.05. **p<0.0001.

Figure 7: Soluble and released BCMA impacts ARI2 activity (See also supplementary movies): (**A**) Measurement of sBCMA from patients with monoclonal gammopathy of undetermined significance (MGUS), MM at diagnosis (Dx) and at relapse. (**B**) Cytotoxicity assay and IFNγ production of ARI2m cells co-cultured with ARP1 MM cells, adding recombinant BCMA protein (BCMA) at 10,000ng/mL (**C**). 24h cytotoxicity assays of ARI2m cells with ARP1 MM cells adding recombinant BCMA at the indicated doses. (**D**) MFI of BCMA and sBCMA (**E**) of ARP1 MM cells alone or in co-culture with either ARI2m or UT T cells with or without DAPT. (**F**) Design of cytotoxic assays in transwell (TW) plates analyzing the impact of sBCMA and DAPT. ARI2m cells and ARP1 cells are co-cultured in the well, and additional ARP1 cells are added in the TW as a source for continuous release of sBCMA. (**G**) Cytotoxicity, IFNγ production and T cell proliferation of experiment designed in (**F**). (**H**) Confocal fluorescence image of MM cells stained with a cell tracker CMAC where BCMA is visualized with a monoclonal anti-BCMA. (**I** and **J**) Time lapse images from two different *in vivo* time lapse experiments over three hours of ARI2m stained with cell tracker CMAC and co-cultured with either RPMI MM cells (**I**) or ARP1 MM cells (**J**) over-expressing BCMA in GFP (See also Supplementary movies 1 and 2). (**K**). Co-

culture assay of T cells with MM-RPMI cells overexpressing BCMA-GFP adding in parallel Latrunculin A. % of T cells acquiring BCMA-GFP in their surface is shown. (**L**). MM-RPMI cells and ARI2m cells were co-cultured for 2 hours to allow transfer of BCMA-GFP to ARI2m cells, then ARI2m cells were sorted and added into a 48h cytotoxicity assays against RPMI-MM cells. *$p<0.05$. **$p<0.0001$.

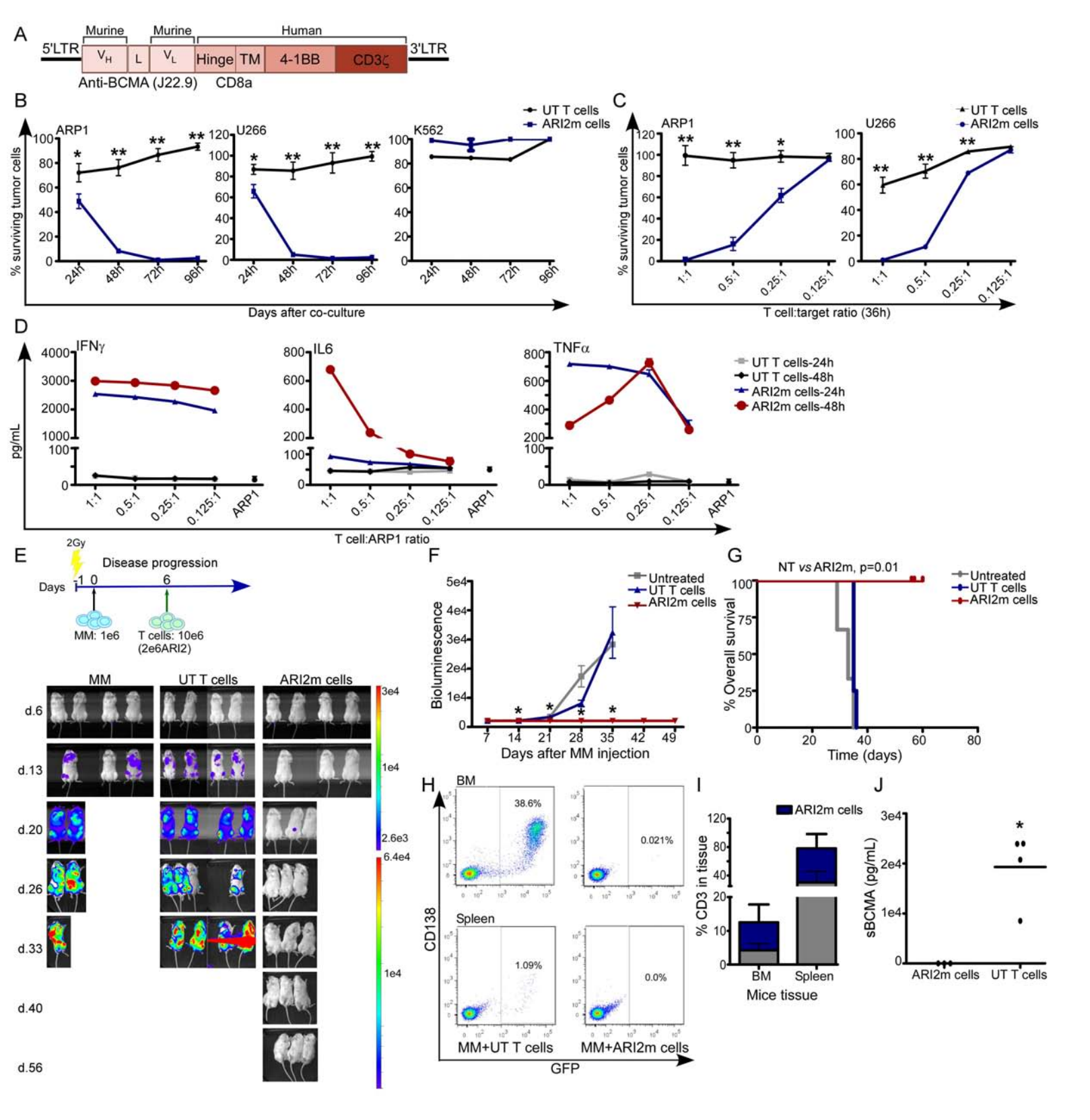
A
Murine
Murine
Human
5'LTR
VH
L
VL
Hinge
TM
4-1BB
CD3ζ
3'LTR
Anti-BCMA (J22.9)
CD8a
B
UT T cells
ARI2m cells
ARP1
U266
K562
% surviving tumor cells
24h
48h
72h
96h
Days after co-culture
C
ARP1
U266
UT T cells
ARI2m cells
% surviving tumor cells
1:1
0.5:1
0.25:1
0.125:1
T cell:target ratio (36h)
D
IFNγ
IL6
TNFα
pg/mL
UT T cells-24h
UT T cells-48h
ARI2m cells-24h
ARI2m cells-48h
T cell:ARP1 ratio
E
2Gy
Disease progression
Days
-1
0
6
MM: 1e6
T cells: 10e6
(2e6ARI2)
MM
UT T cells
ARI2m cells
d.6
d.13
d.20
d.26
d.33
d.40
d.56
3e4
1e4
2.6e3
6.4e4
1e4
F
Untreated
UT T cells
ARI2m cells
Bioluminescence
Days after MM injection
G
NT vs ARI2m, p=0.01
Untreated
UT T cells
ARI2m cells
% Overall survival
Time (days)
H
BM
Spleen
38.6%
0.021%
1.09%
0.0%
CD138
MM+UT T cells
MM+ARI2m cells
GFP
I
ARI2m cells
% CD3 in tissue
BM
Spleen
Mice tissue
J
sBCMA (pg/mL)
ARI2m cells
UT T cells

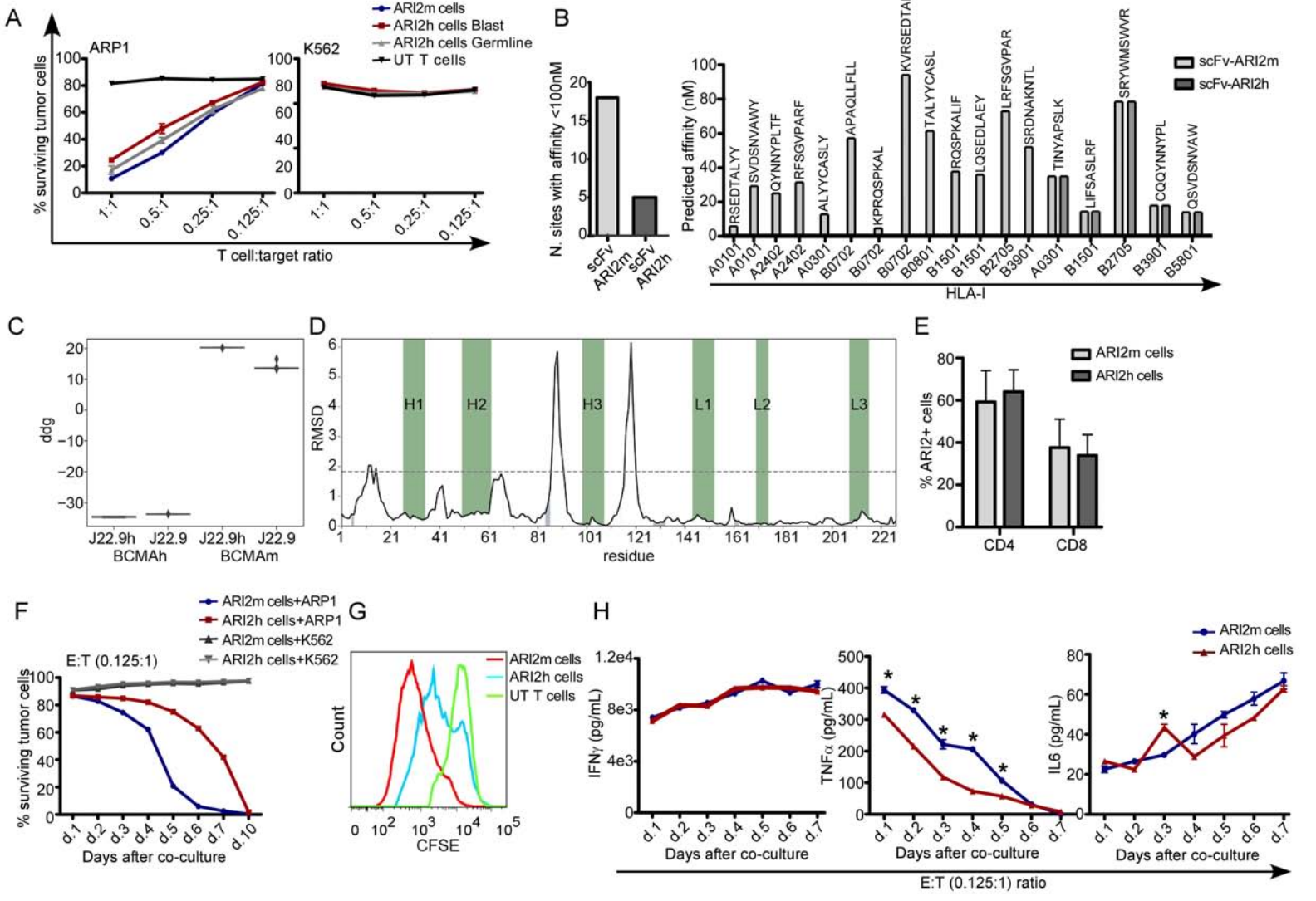
A
ARI2m cells
ARI2h cells Blast
ARI2h cells Germline
UT T cells
ARP1
K562
% surviving tumor cells
T cell:target ratio
1:1
0.5:1
0.25:1
0.125:1
B
N. sites with affinity <100nM
scFv ARI2m
scFv ARI2h
Predicted affinity (nM)
scFv-ARI2m
scFv-ARI2h
RSEDTALYY
SVDSNVAWY
QYNNYPLTF
RFSGVPARF
ALYYCASLY
APAQLLFLL
KPRQSPKAL
KVRSEDTAL
TALYYCASL
RQSPKALIF
LQSEDLAEY
LRFSGVPAR
SRDNAKNTL
TINYAPSLK
LIFSASLRF
SRYWMSWVR
CQQYNNYPL
QSVDSNVAW
A0101
A0101
A2402
A2402
A0301
B0702
B0702
B0702
B0801
B1501
B1501
B2705
B3901
A0301
B1501
B2705
B3901
B5801
HLA-I
C
ddg
J22.9h
J22.9
J22.9h
J22.9
BCMAh
BCMAm
D
RMSD
H1
H2
H3
L1
L2
L3
residue
E
ARI2m cells
ARI2h cells
% ARI2+ cells
CD4
CD8
F
ARI2m cells+ARP1
ARI2h cells+ARP1
ARI2m cells+K562
ARI2h cells+K562
E:T (0.125:1)
% surviving tumor cells
Days after co-culture
G
ARI2m cells
ARI2h cells
UT T cells
Count
CFSE
H
ARI2m cells
ARI2h cells
IFNγ (pg/mL)
TNFα (pg/mL)
IL6 (pg/mL)
Days after co-culture
E:T (0.125:1) ratio

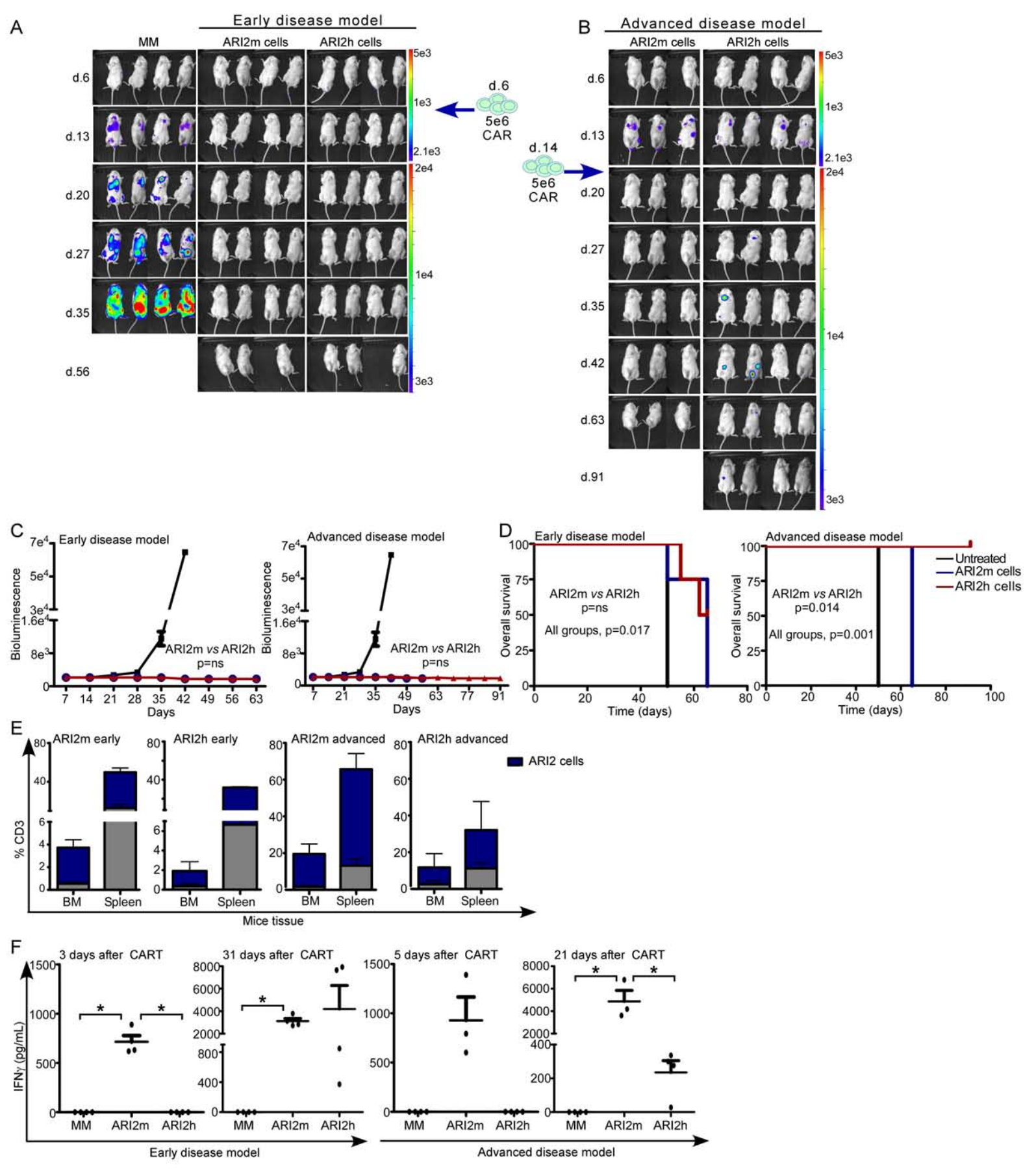
A
Early disease model
MM
ARI2m cells
ARI2h cells
d.6
d.13
d.20
d.27
d.35
d.56
5e3
1e3
2.1e3
2e4
1e4
3e3
d.6
5e6
CAR
d.14
5e6
CAR
B
Advanced disease model
ARI2m cells
ARI2h cells
d.6
d.13
d.20
d.27
d.35
d.42
d.63
d.91
5e3
1e3
2.1e3
2e4
1e4
3e3
C
Early disease model
Advanced disease model
Bioluminescence
ARI2m vs ARI2h
p=ns
Days
D
Early disease model
Advanced disease model
Overall survival
ARI2m vs ARI2h
p=ns
All groups, p=0.017
ARI2m vs ARI2h
p=0.014
All groups, p=0.001
Time (days)
Untreated
ARI2m cells
ARI2h cells
E
ARI2m early
ARI2h early
ARI2m advanced
ARI2h advanced
ARI2 cells
% CD3
BM
Spleen
Mice tissue
F
3 days after CART
31 days after CART
5 days after CART
21 days after CART
IFNγ (pg/mL)
MM
ARI2m
ARI2h
Early disease model
Advanced disease model

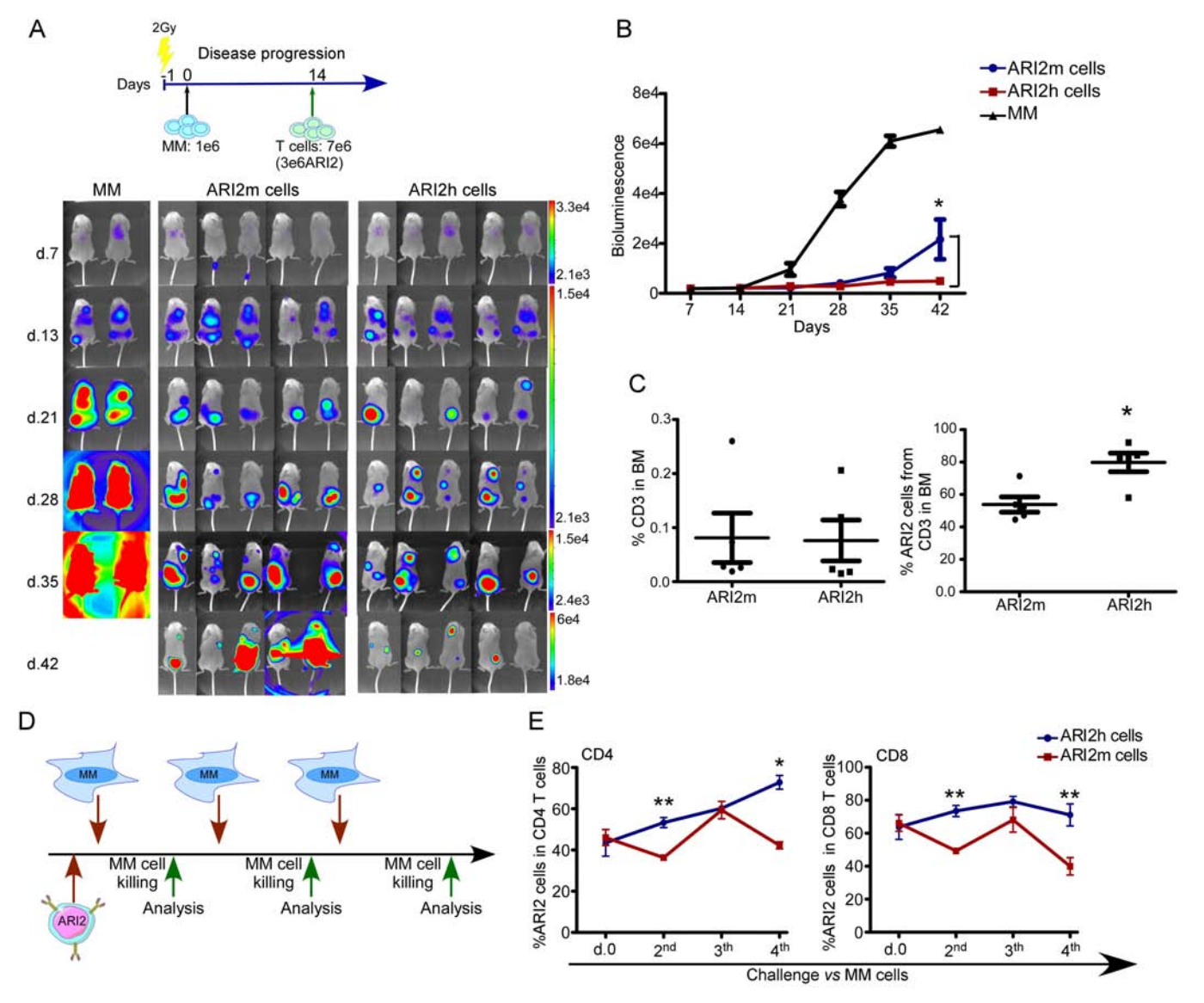
A
2Gy
Disease progression
Days
-1
0
14
MM: 1e6
T cells: 7e6
(3e6ARI2)
MM
ARI2m cells
ARI2h cells
d.7
d.13
d.21
d.28
d.35
d.42
3.3e4
2.1e3
1.5e4
2.1e3
1.5e4
2.4e3
6e4
1.8e4
B
ARI2m cells
ARI2h cells
MM
Bioluminescence
8e4
6e4
4e4
2e4
0
7
14
21
28
35
42
Days
*
C
% CD3 in BM
0.3
0.2
0.1
0.0
ARI2m
ARI2h
% ARI2 cells from CD3 in BM
100
80
60
40
20
0.0
*
ARI2m
ARI2h
D
MM
MM
MM
MM cell killing
Analysis
MM cell killing
Analysis
MM cell killing
Analysis
ARI2
E
ARI2h cells
ARI2m cells
CD4
%ARI2 cells in CD4 T cells
80
60
40
20
0
**
*
d.0
2nd
3th
4th
CD8
%ARI2 cells in CD8 T cells
100
80
60
40
20
0
**
**
d.0
2nd
3th
4th
Challenge vs MM cells

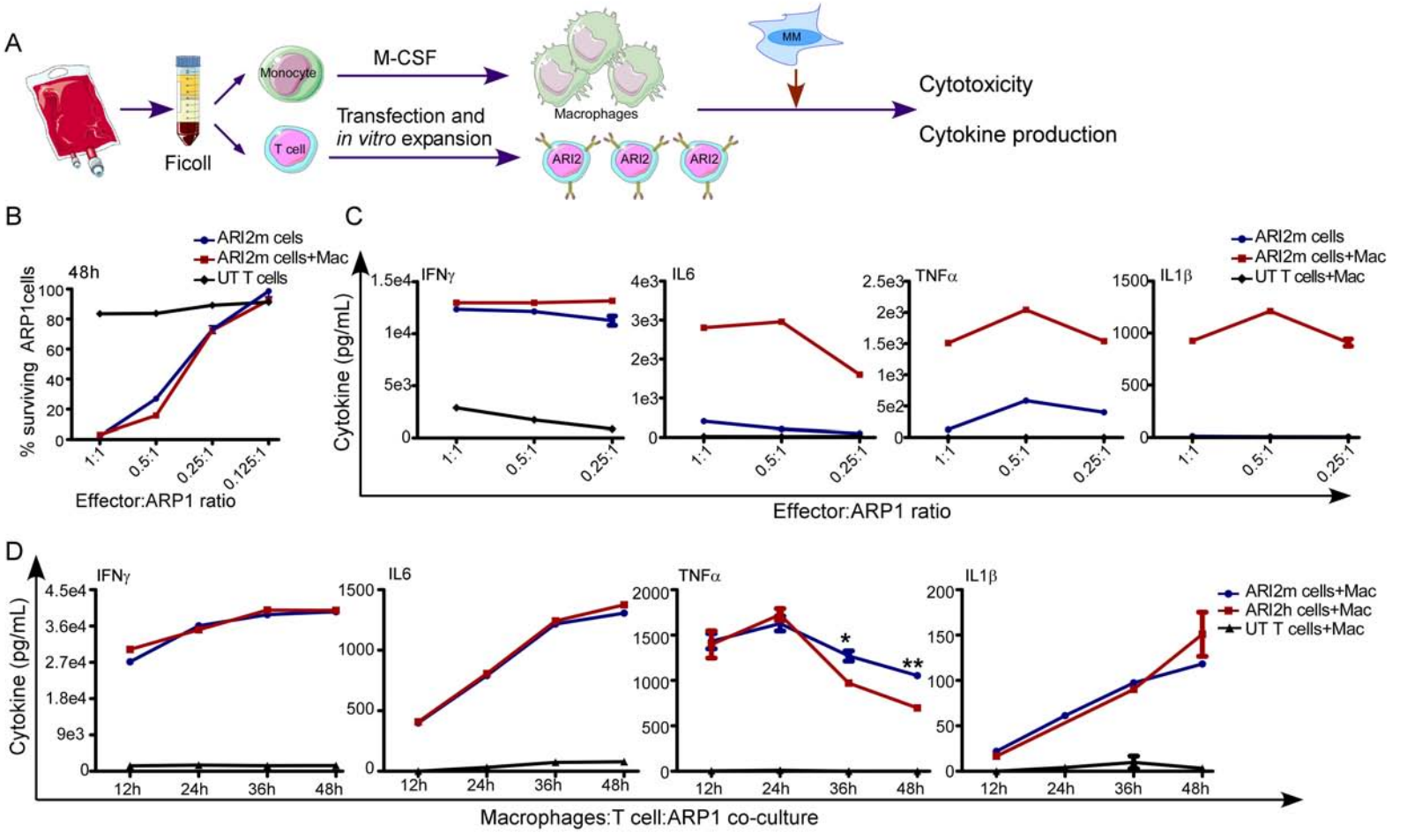
A
Ficoll
Monocyte
T cell
M-CSF
Transfection and
in vitro expansion
Macrophages
ARI2
ARI2
ARI2
MM
Cytotoxicity
Cytokine production
B
48h
ARI2m cels
ARI2m cells+Mac
UT T cells
% surviving ARP1cells
Effector:ARP1 ratio
C
ARI2m cells
ARI2m cells+Mac
UT T cells+Mac
IFNγ
IL6
TNFα
IL1β
Cytokine (pg/mL)
Effector:ARP1 ratio
D
IFNγ
IL6
TNFα
IL1β
ARI2m cells+Mac
ARI2h cells+Mac
UT T cells+Mac
Cytokine (pg/mL)
Macrophages:T cell:ARP1 co-culture

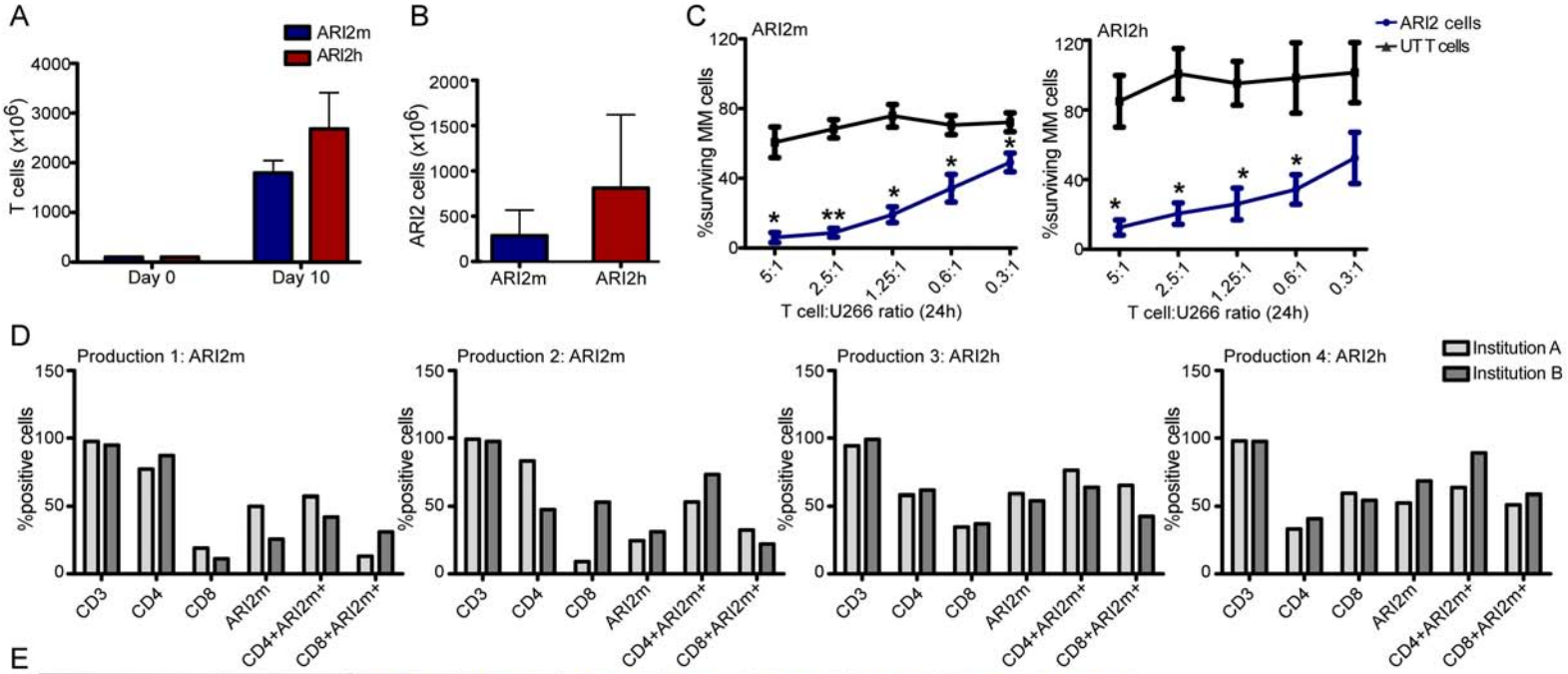

E

Parameter	Limit	ARI2m (Inst. A)	ARI2m (Inst. A)	ARI2m (Inst. B)	ARI2m (Inst. B)	ARI2h (Inst. A)	ARI2h (Inst. A)	ARI2h (Inst. B)	ARI2h (Inst. B)
Viability	≥70%	95%	92%	96%	92.8%	95%	92%	98.7%	89.28%
Sterility	Sterile	Sterile	Sterile	Sterile	Sterile	Sterile	Sterile	Sterile	Sterile
Endotoxins	≤0.5 UE/mL	<0.5	<0.5	<0.5	<0.5	<0.5	<0.5	<0.5	<0.5
Mycoplasma	Absent	Absent	Absent	Absent	Absent	Absent	Absent	Absent	Absent
N. of integrations	≤10	7.41	7.3	1.71	1.89	4.56	3.72	0.78	2.95
% ARI2 cells	>15%	49.9	24.6	25.62	31.21	58.6	52.4	54.08	68.32
Total ARI2 cells	>180 (x10^6)	698	344	625	605	940	1572	2498	1024

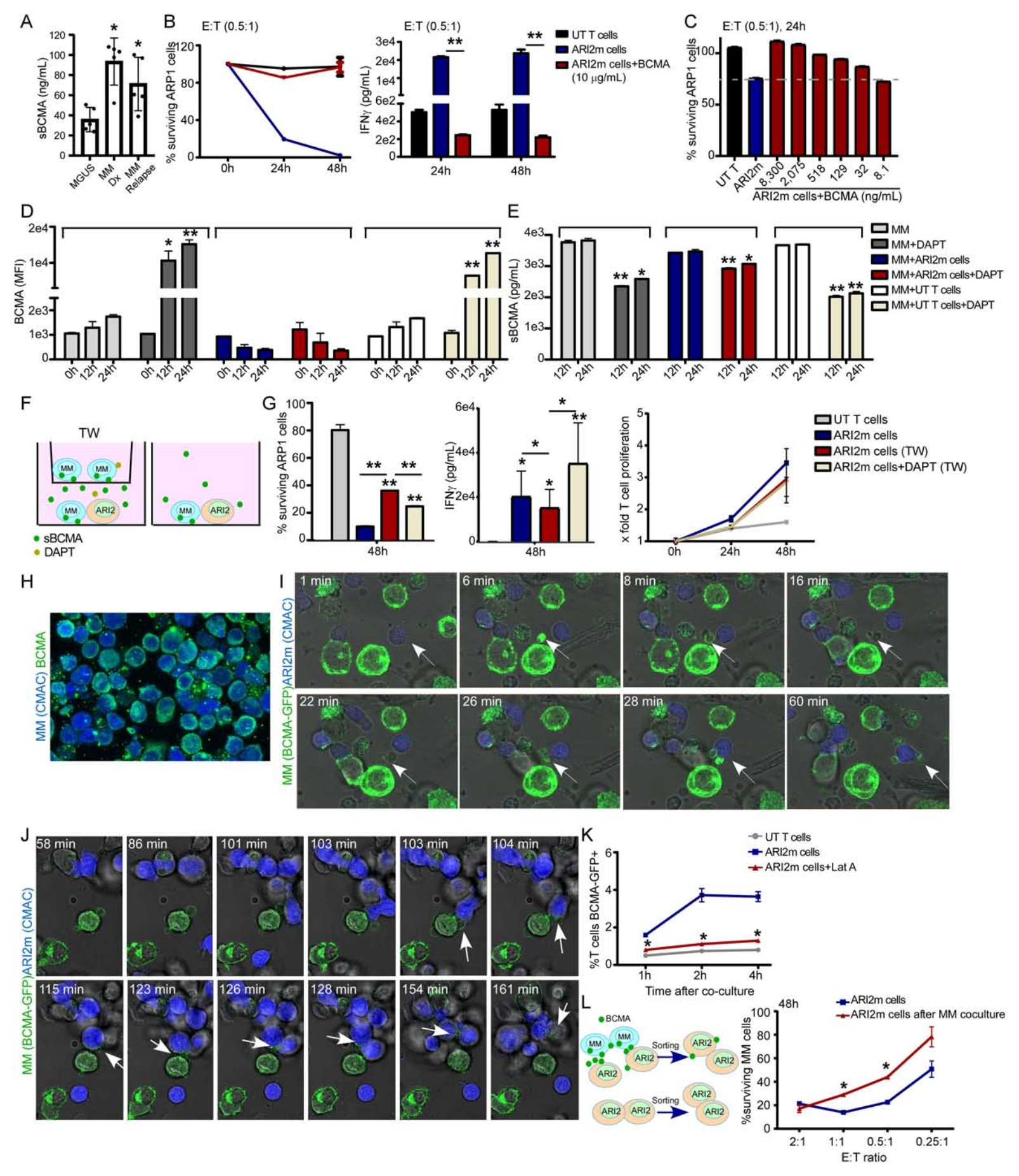
A
sBCMA (ng/mL)
MGUS
MM Dx
MM Relapse
B
E:T (0.5:1)
% surviving ARP1 cells
0h
24h
48h
E:T (0.5:1)
IFNγ (pg/mL)
UT T cells
ARI2m cells
ARI2m cells+BCMA (10 μg/mL)
C
E:T (0.5:1), 24h
% surviving ARP1 cells
UT T
ARI2m
8,300
2,075
518
129
32
8.1
ARI2m cells+BCMA (ng/mL)
D
BCMA (MFI)
0h 12h 24h
E
sBCMA (pg/mL)
MM
MM+DAPT
MM+ARI2m cells
MM+ARI2m cells+DAPT
MM+UT T cells
MM+UT T cells+DAPT
F
TW
MM
ARI2
sBCMA
DAPT
G
% surviving ARP1 cells
48h
IFNγ (pg/mL)
× fold T cell proliferation
UT T cells
ARI2m cells
ARI2m cells (TW)
ARI2m cells+DAPT (TW)
H
MM (CMAC) BCMA
I
MM (BCMA-GFP)ARI2m (CMAC)
1 min
6 min
8 min
16 min
22 min
26 min
28 min
60 min
J
MM (BCMA-GFP)ARI2m (CMAC)
58 min
86 min
101 min
103 min
103 min
104 min
115 min
123 min
126 min
128 min
154 min
161 min
K
%T cells BCMA-GFP+
UT T cells
ARI2m cells
ARI2m cells+Lat A
Time after co-culture
L
BCMA
Sorting
ARI2
%surviving MM cells
48h
ARI2m cells
ARI2m cells after MM coculture
E:T ratio

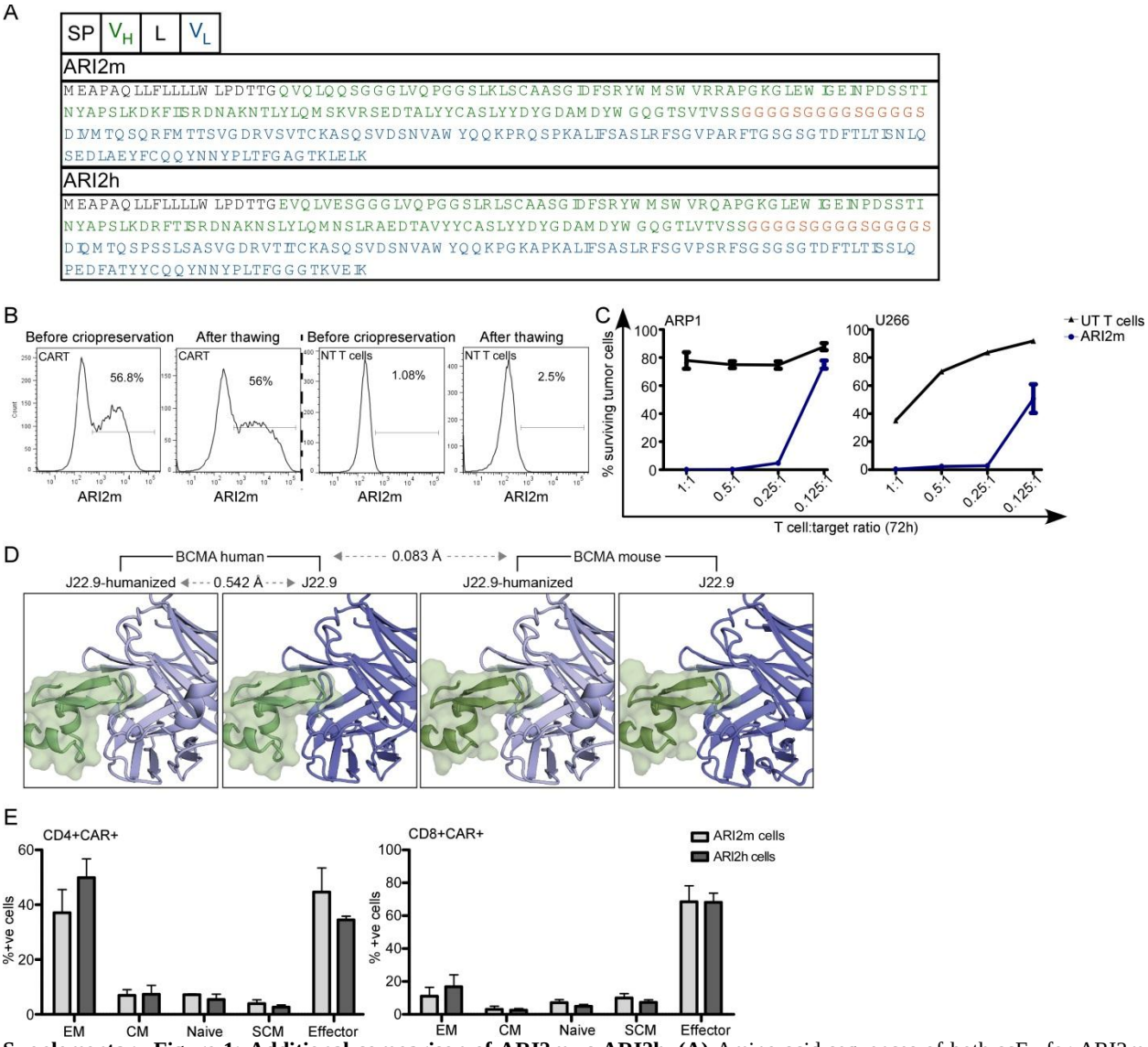

Supplementary Figure 1: Additional comparison of ARI2m *vs* ARI2h. (A) Amino acid sequences of both scFv for ARI2m and ARI2h. **(B)** Percentage of ARI2m cells before and after cryopreservation. UT T cells are shown as control. **(C)** Limiting dilution cytotoxicity assay of ARI2m and UT T cells *vs* MM cells (ARP1 and U266). (**D**). Protein-protein interfaces between the two scFv variants (J22.9 and J22.9h) and the two BCMA homologues. Root Mean Square Deviation (RMSD) between variants is annotated. (**E**). Phenotype characterization of T cells transduced with either ARI2m or ARI2h CAR construct and after being expanded for 7 days (n=3). EM (effector memory), CM (central memory), SCM (stem cell memory).

Supplementary Movie 1: live time lapse images of ARI2m cells stained in blue (CMAC) and RPMI-MM cells overexpressing BCMA fused to green fluorescent protein (GFP). Images were acquired every 20 seconds using a Leica SP5 confocal microscopy.

Supplementary Movie 2: live time lapse images of ARI2m cells stained in blue (CMAC) and ARP1-MM cells overexpressing BCMA fused to green fluorescent protein (GFP). Images were acquired every 20 seconds using a Leica SP5 confocal microscopy.

Supplementary methods:

Cell cultures: RPMI8226, U266 and K562 cell lines were purchased from American Tissue Culture Collection (ATCC, Manassas, VA). ARP1 cell line was kindly provided by Multiple Myeloma Research Center (Little Rock, AK, USA). Cell lines K562, RPMI8226 and ARP1 were cultured in RPMI with 10% Fetal Bovine Serum (FBS) and 1% Penicillin/streptomycin (Pen/Strep) and U266 with 15% FBS. HEK293-T cells were cultured with DMEM with 10% FBS and 1% Pen/Strep.

Virus production and T cell transfection: HEK293-T cells were transfected with lentiviral vectors (pCCL-EF1α-BCMA, pREV-REV, pMDLg/pRRE and pCMV-VSV-G). Lentiviral supernatant was collected 48 hours later and concentrated with LentiX-Concentrator (Clontech, Takara) following the manufacturer's protocol. Concentrated lentivirus was kept at -80ºC until use. T cells from healthy donors were activated on day 0 with CD3/CD28 Dynabeads and transduced with concentrated lentivirus on day 2 in media containing Polybrene (Merck Millipore). Spinoculation was performed using centrifugation at 2,000 rpm for 1hour.

CART cell expansion: Lymphocytes were obtained by Ficoll and magnetic T cell depletion (Miltenyi Biotec). T cells were expanded in Click's media (50% RPMI, 50% Click's (Irvine Scientific), 5% human Serum and 1% Pen/strep), activated with Dynabeads Human T-Activator CD3/CD28 (Thermo Fisher Scientific) and IL-2 (100 IU/mL) every other day. Experiments were performed after 8-10 days of T cell expansion.

Flow cytometry: CAR-BCMA was detected with a recombinant BCMA-Fc protein (Enzo Life Sciences) and a secondary antibody anti-human IgG Fc conjugated to Brilliant Violet (BV)-421 (Biolegend). Antibodies used were CD3-APC, CD8-PeCy7 and CD4-APCH7 (Becton Dickinson). Memory subsets were identified with CD45Ra-APC (Biolegend), CCR7-BV510 and CXCR3-Alx-488 (BD biosciences). MM cells were stained with CD138-BV421 (Becton Dickinson) and BCMA-APC (Biolegend). Flow cytometry analysis was performed using FlowJo software.

Cytotoxicity: Assays were performed using different effector:target ratios and at different time-points. Target cells used in these assays had been previously modified with a lentiviral vector to over-express GFP-firefly luciferase (GFP-ffLuc). Percentage of remaining live GFP+ tumor cells was analyzed by flow cytometry according to the following formula: % of live cell=100x(N. of GFP+ cells with T cells at time x /N of GFP+ cells alone at time x).

Immunogenicity prediction: NetMHC uses an approximation algorithm that reliably predicts the affinity of peptides of lengths 8, 10 and 11, for which affinity data for training are rare. The method uses predictors trained on peptides of length 9 to successfully extrapolate to other lengths. In short, the method approximates each peptide of any length to a number of 9-mers, by inserting X (for 8-mers) or deleting amino acid(s) (for 10- and 11-mers) and set the final prediction to an average of the 9-mer predictions. Bind Level indicates if the peptide is predicted to bind stronger than a certain threshold. Predicted affinities weaker than 500 nM or lower than the 1% percentile score have no indications [1-3].

***In vivo* myeloma murine model**: 8-12 weeks old NOD/SCID IL-2Rcnull (NSG) mice were irradiated at 2Gy at day -1. At day 0, mice received i.v. 1-1.5 $x10^6$ GFP-ffLuc-ARP-1 cells. Either at day 6 or day 14, depending on the disease model, mice received i.v. either untransduced (UT) T cells or CART cells. Mice were subjected to weekly bioluminescence imaging (BLI) using a Hamamatsu color CDD camera (Hamamatsu Photonics Systems, Bridgewater, NJ) following IP injection of D-luciferin (20 mg/mL PBS). Signal was quantified using Image J software.

Proliferation assays: CART cells were stained with CellTrace™ CFSE Cell Proliferation Kit (Invitrogen, Thermo Fisher Scientific) before being co-cultured under different conditions and cell lines for 96 hours. Proliferation was analyzed by Flow cytometry.

Cytokine production and sBCMA: IFN-γ, TNF-α, IL-6, IL-1β cytokines were quantified by ELISAs (ELISA MAX™ Deluxe Set, Biolegend) following manufacturer's protocol. Soluble BCMA was detected by ELISA (Human BCMA/TNFRSF17 DuoSet ELISA, R&D systems) following manufacturer's protocol.

Macrophage differentiation: After performing Ficoll, monocytes were isolated with RosetteSep Human Monocyte Enrichment Cocktail (Stem Cell Technologies) and macrophages were differentiated from monocytes after 1 week expansion with RPMI 10% FBS and 0.1mg/ml M-CSF (Thermo Fisher Scientific).

Confocal microscopy: RPMI cell line overexpressing BCMA fused to green fluorescent protein (GFP) was generated and then co-cultured with CART cells stained with Cell Tracker™ Blue CMAC Dye (Thermo Fisher Scientific). BCMA was also detected by confocal fluorescence microscopy with monoclonal anti-TNRSF17 mouse antibody (Sigma-Aldrich) and secondary anti-mouse IgG Alexa 647 (Cell signaling Technologies). Images were acquired using a Leica SP5 microscope. 405, 488 and 633 lasers were used for excitation. For time lapse experiments, *in vivo* image acquisitions were performed every 20 seconds.

References:

1. Lundegaard C, Lamberth K, Harndahl M, Buus S, Lund O, Nielsen M. NetMHC-3.0: accurate web accessible predictions of human, mouse and monkey MHC class I affinities for peptides of length 8-11. Nucleic Acids Res. 2008;36(Web Server issue):W509-512.
2. Andreatta M, Nielsen M. Gapped sequence alignment using artificial neural networks: application to the MHC class I system. Bioinformatics. 2016;32(4):511-517.
3. Nielsen M, Andreatta M. NetMHCpan-3.0; improved prediction of binding to MHC class I molecules integrating information from multiple receptor and peptide length datasets. Genome Med. 2016;8(1):33.